



RESEARCH ARTICLE

10.1002/2014JD022697

Key Points:

- CH₄ emissions from Haynesville, Fayetteville, and Marcellus regions quantified
- CH₄ emissions similar to previously studied gas-producing regions
- CH₄ loss rates lower than previously studied gas-producing regions

Correspondence to:

J. Peischl,
jeff.peischl@noaa.gov

Citation:

Peischl, J., et al. (2015), Quantifying atmospheric methane emissions from the Haynesville, Fayetteville, and northeastern Marcellus shale gas production regions, *J. Geophys. Res. Atmos.*, 120, 2119–2139, doi:10.1002/2014JD022697.

Received 8 OCT 2014

Accepted 9 FEB 2015

Accepted article online 18 FEB 2015

Published online 13 MAR 2015

Corrected 1 APR 2015

This article was corrected on 1 APR 2015.
See the end of the full text for details.

Quantifying atmospheric methane emissions from the Haynesville, Fayetteville, and northeastern Marcellus shale gas production regions

J. Peischl^{1,2}, T. B. Ryerson², K. C. Aikin^{1,2}, J. A. de Gouw^{1,2}, J. B. Gilman^{1,2}, J. S. Holloway^{1,2}, B. M. Lerner^{1,2}, R. Nadkarni³, J. A. Neuman^{1,2}, J. B. Nowak^{1,2,4}, M. Trainer², C. Warneke^{1,2}, and D. D. Parrish^{1,2}

¹Cooperative Institute for Research in Environmental Sciences, University of Colorado Boulder, Boulder, Colorado, USA,

²Chemical Sciences Division, NOAA Earth System Research Laboratory, Boulder, Colorado, USA, ³Texas Commission on Environmental Quality, Austin, Texas, USA, ⁴Now at Aerodyne Research, Inc., Billerica, Massachusetts, USA

Abstract We present measurements of methane (CH₄) taken aboard a NOAA WP-3D research aircraft in 2013 over the Haynesville shale region in eastern Texas/northwestern Louisiana, the Fayetteville shale region in Arkansas, and the northeastern Pennsylvania portion of the Marcellus shale region, which accounted for the majority of Marcellus shale gas production that year. We calculate emission rates from the horizontal CH₄ flux in the planetary boundary layer downwind of each region after subtracting the CH₄ flux entering the region upwind. We find 1 day CH₄ emissions of $(8.0 \pm 2.7) \times 10^7$ g/h from the Haynesville region, $(3.9 \pm 1.8) \times 10^7$ g/h from the Fayetteville region, and $(1.5 \pm 0.6) \times 10^7$ g/h from the Marcellus region in northeastern Pennsylvania. Finally, we compare the CH₄ emissions to the total volume of natural gas extracted from each region to derive a loss rate from production operations of 1.0–2.1% from the Haynesville region, 1.0–2.8% from the Fayetteville region, and 0.18–0.41% from the Marcellus region in northeastern Pennsylvania. The climate impact of CH₄ loss from shale gas production depends upon the total leakage from all production regions. The regions investigated in this work represented over half of the U.S. shale gas production in 2013, and we find generally lower loss rates than those reported in earlier studies of regions that made smaller contributions to total production. Hence, the national average CH₄ loss rate from shale gas production may be lower than values extrapolated from the earlier studies.

1. Introduction

Natural gas accounted for 30% of the energy produced in the United States (U.S.) in 2013 [U.S. Energy Information Administration (EIA), www.eia.gov]. So-called unconventional shale gas extraction, using directional drilling and hydraulic fracturing, has become a major source of natural gas in recent years (Figure 1); as of June 2013, unconventional natural gas extracted from shale formations accounted for 40% of the nation's total natural gas extraction. Current EIA estimates place the total recoverable shale gas in the world at over 2×10^{14} m³ (7 quadrillion cubic feet, <http://www.eia.gov/todayinenergy/detail.cfm?id=116111>), which at 2013 natural gas consumption rates would take the U.S. approximately 260 years to consume, making shale gas a significant source of energy for the future.

Natural gas is a mixture primarily composed of methane (CH₄) with C₂–C₅ alkanes, nitrogen (N₂), and carbon dioxide (CO₂) typically making up the balance. The relative abundances of these alkanes depend on the geologic formation from which it was extracted; natural gas associated with oil deposits is typically wetter, i.e., has more C₂–C₅ alkanes relative to CH₄ than natural gas not associated with oil deposits. Most natural gas, once extracted from the ground, requires additional processing before it is ready to be used as a fuel. This processing includes removing any water (H₂O) from the gas and removing the C₂–C₅ alkanes for their use separately as fuel and chemical feedstocks. The result of this processing is called dry natural gas, which is composed mainly of CH₄, with C₂₊ alkanes typically making up less than 5% of the gas by volume. Dry natural gas is then compressed and transported through pipelines for use downstream in residential, commercial, electrical, and industrial applications. Here we use the term “production” in an operational sense to refer to upstream natural gas extraction, processing, and compression operations within specific geographic areas sampled by our atmospheric measurements.

This is an open access article under the terms of the Creative Commons Attribution-NonCommercial-NoDerivs License, which permits use and distribution in any medium, provided the original work is properly cited, the use is non-commercial and no modifications or adaptations are made.

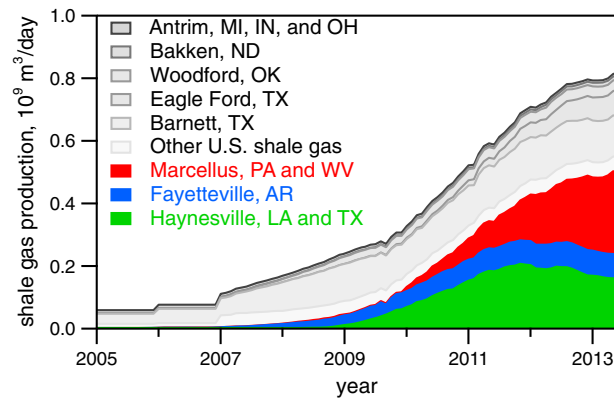


Figure 1. Unconventional shale gas production from various shale plays through June 2013. Source: U.S. Energy Information Administration (downloaded December 2013).

natural-gas-based energy supply [e.g., *Hayhoe et al.*, 2002]. Here we summarize recent work published since the boom in shale gas production in the late 2000s. *Howarth et al.* [2011] estimated that a total loss rate, from extraction through end use, above 2–3% would offset the climate benefits of using natural gas as a fuel instead of oil or coal. *Howarth et al.* [2011] further summed bottom-up estimates of loss rates for various stages of shale gas production and estimated that 3.6–7.9% of the natural gas extracted from shale is lost to the atmosphere over the lifetime of a shale gas well. They estimated that 1.9% of the natural gas is lost during the well completion stage, and 0.3–1.9% is lost during routine operations of a well. However, *Cathles et al.* [2012] argued that the loss rates used by Howarth et al. for some stages of the natural gas production were too high by up to a factor of 10 and concluded that the net climate impact of natural gas is a factor of 2–3 less than that of coal. *Wigley* [2011] examined different scenarios of switching from coal to natural gas as a power plant fuel and concluded that a total natural gas loss rate below 2% would reduce the net CH₄ emissions to the atmosphere, but that loss rates as high as 10% would still prove beneficial after many years because of the increased efficiency of, and decreased black carbon emissions from, natural-gas-fired power plants when compared to coal-fired power plants throughout the world. *Alvarez et al.* [2012] concluded that a total natural gas loss rate below 3.2% represented an immediate climate benefit if natural gas were to replace coal as fuel for power plants. Ultimately, the total end-to-end loss rates from natural gas production and consumption have implications for future fuel choices and climate change mitigation, and top-down estimates of CH₄ emissions from natural gas production regions are critically needed to verify bottom-up emissions estimates upon which climate policy decisions are based.

Studies using atmospheric measurements have only recently constrained CH₄ emissions to the atmosphere from natural gas production in source regions. Several of these studies have estimated CH₄ emissions using ambient measurements and calculated a loss rate by dividing these CH₄ emissions by the total CH₄ from natural gas produced in the region. *Pétron et al.* [2012] estimated natural gas losses to the atmosphere in 2008 equal to 3.1–5.3% of production from the Denver-Julesburg Basin in northeastern Colorado, a region that accounted for approximately 0.9% of U.S. natural gas production in 2008. *Pétron et al.* [2014] revisited the Denver-Julesburg Basin in 2012 and, using a different approach, again concluded that $(4.1 \pm 1.5)\%$ of the natural gas produced in the region was emitted to the atmosphere. *Karion et al.* [2013] estimated a 6.2–11.7% loss from natural gas production in the Uinta Basin in northeastern Utah, a region that accounted for approximately 1.0% of U.S. natural gas production in February 2012. *Peischl et al.* [2013] estimated a $(17 \pm 5)\%$ loss from natural gas production in the Los Angeles basin in California, a region of very low production (approximately 0.05% of U.S. natural gas production in 2010). *Caulton et al.* [2014] found loss rates of 2.8–17.3% for two June 2012 flights in the southwestern Pennsylvania region of the Marcellus shale at a time when that region accounted for approximately 2.7% of U.S. natural gas production. Each of these loss rate determinations was significantly greater than the U.S. Environmental Protection Agency [2014] estimates for the loss rate from production in 2008, which ranged from 0.16% to 1.47% [*Karion et al.*, 2013]. In contrast, *Allen et al.* [2013] measured CH₄ emissions from different stages of natural gas production from hundreds of wells across the U.S. and found that the losses from production operations, 0.42%, were similar to the Environmental Protection Agency (EPA) estimate of 0.47% in 2011. The wide range of natural gas loss estimates indicates that further investigation of this issue is

Natural gas is a more efficient fuel for power plants than coal, resulting in a lower CO₂ emission per unit of energy produced [e.g., see *de Gouw et al.*, 2014]. However, CH₄ is 28 times more potent a greenhouse gas than CO₂ on a 100 year time horizon [*Myhre et al.*, 2013]. Therefore, the amount of natural gas, and thus CH₄, that is emitted to the atmosphere before it is burned as a fuel has a significant effect on the net climate impact of using natural gas for energy production. Many published works have analyzed the climate impacts of CH₄ emissions from natural gas production by comparing the net effects on the radiative forcing of the atmosphere between a coal-based versus

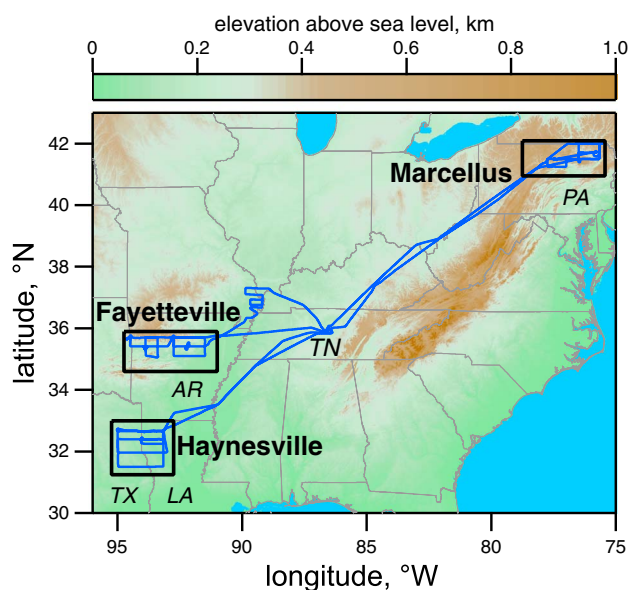


Figure 2. Map of the three study areas. The black rectangles show the insets for the maps of the Haynesville, Fayetteville, and Marcellus shale regions shown in Figures 3, 7, and 9, respectively. The blue traces show three of the flight tracks of the NOAA P-3 during SENEX.

shale gas in the U.S. Since the end of 2011, production decreased to approximately $1.6 \times 10^8 \text{ m}^3$ (5.6 billion cubic feet) per day by June 2013, when it accounted for 6.9% of U.S. natural gas production and 19.5% of U.S. unconventional shale gas production. This region accounted for 8.5% of June 2013 U.S. natural gas production when production from formations in the region other than the Haynesville shale is included. The second region we examine is the Fayetteville shale play located in central Arkansas. Unconventional natural gas production from the Fayetteville shale began in 2007, peaked in late 2012, and was $7.6 \times 10^7 \text{ m}^3$ (2.7 billion cubic feet) per day in June 2013, when it accounted for 3.4% of U.S. natural gas production and 9.5% of U.S. unconventional shale gas production. The third region we examine is a portion of the Marcellus shale play located in northeastern Pennsylvania where unconventional drilling predominates. Natural gas production from the Marcellus shale has increased steadily since early 2010. By June 2013, production from the entire Marcellus shale formation was over $2.6 \times 10^8 \text{ m}^3$ (9.2 billion cubic feet) per day, which made it the largest shale-gas-producing play in the U.S. The northeastern Pennsylvania portion of the Marcellus shale play accounted for approximately 70% of the total Marcellus production, as discussed in more detail below. In June 2013, the northeastern Pennsylvania portion of the Marcellus shale play accounted for approximately 8.0% of U.S. natural gas production and 22.5% of U.S. unconventional shale gas production.

We estimate the total CH_4 emission to the atmosphere from these regions using measurements taken aboard the chemically instrumented National Oceanic and Atmospheric Administration (NOAA) WP-3D (P-3) aircraft in the summer of 2013 during the Southeast Nexus (SENEX) field campaign, based out of Smyrna, Tennessee (Figure 2). Using a mass balance approach, we calculate the horizontal flux of CH_4 through the planetary boundary layer (PBL) downwind of the Haynesville, Fayetteville, and a portion of the Marcellus shale regions. In cases with full upwind transects, we calculate the CH_4 flux flowing into the region, and the difference between the upwind and downwind fluxes provides an estimate of the CH_4 emissions from the region. Otherwise, we use the downwind transect only with an increased uncertainty in the upwind background CH_4 mixing ratio to derive an emissions estimate. We then divide this emission by the natural gas production to derive a loss rate from natural gas production in each region.

2. Instrumentation

CH_4 , C_2 – C_5 alkanes, ammonia (NH_3), carbon monoxide (CO), and meteorological measurements, among many others, were made aboard an instrumented NOAA P-3 research aircraft during June and July 2013 for

necessary. These studies provide key top-down information on CH_4 losses from production, processing, and distribution in source regions, to which CH_4 losses from downstream natural gas distribution and use must be added before comparing total climate impacts to coal.

Here we derive atmospheric CH_4 emission rates from three natural gas production regions, which together accounted for over 50% of the unconventional shale gas produced in the U.S. and approximately 20% of the entire U.S. natural gas production in June 2013. The first region we examine is the Haynesville shale play located in eastern Texas and northwestern Louisiana. Unconventional natural gas production from the Haynesville shale increased steadily from late 2008 until late 2011, when it reached $2.1 \times 10^8 \text{ m}^3$ (7 billion cubic feet) per day (EIA) (Figure 1). At that time, the field was the largest producer of unconventional

the SENEX field campaign. CH₄ was measured with a Picarro 1301-m once per second with an estimated accuracy of ± 1.2 ppb (all uncertainties herein are 1σ); 1 s precision was ± 1.5 ppb [Peischl *et al.*, 2012]. All CH₄ units herein are dry air mole fractions of nanomole/mole, or ppb. Ethane was measured with an estimated accuracy of $\pm 19\%$ in whole air sample canisters [Colman *et al.*, 2001], which typically took about 10 s to fill. In addition to ethane, hydrocarbons such as propane, *n*- and *i*-butane, and *n*- and *i*-pentane were measured in the whole air samples, as well as aromatics such as benzene and toluene. NH₃ was measured by chemical ionization mass spectrometry with an estimated accuracy of $\pm (25\% + 80$ parts per trillion by volume (pptv)) and a 1 s precision of ± 30 pptv [Nowak *et al.*, 2007]. CO was measured by vacuum ultraviolet resonance fluorescence with an estimated accuracy of $\pm 5\%$ and a 1 s precision of ± 1 parts per billion by volume (ppbv) [Holloway *et al.*, 2000]. Meteorological and navigational data were measured once per second by various sensors aboard the NOAA P-3. We estimate the uncertainties for these measurements as follows: wind speed (± 1 m/s), wind direction ($\pm 5^\circ$), ambient temperature ($\pm 0.5^\circ\text{C}$), potential temperature (θ , ± 0.5 K), dew point ($\pm 0.5^\circ\text{C}$), heading ($\pm 0.5^\circ$), radar altitude (± 15 m), GPS altitude (± 16 m), H₂O ($\pm 5\%$ in units of g/kg), and ground speed (± 3.4 m/s). We additionally derive the virtual potential temperature ($\theta_v = \theta \times [1 + 0.61 \times \text{H}_2\text{O}/1000]$) for use during vertical profiles to help define the depth of the planetary boundary layer (PBL), and the terrain height directly below the P-3 (= GPS altitude – radar altitude). One sigma estimates of the uncertainty in wind speed and direction along a P-3 transect are calculated using the method of Yamartino [1984].

3. Other Data

Louisiana well locations were obtained from the Louisiana Department of Natural Resources Web site (<http://dnr.louisiana.gov/index.cfm?md=pagebuilder&tmp=home&pid=442>, accessed November 2013). Louisiana well production data were obtained from the State of Louisiana Department of Natural Resources Strategic Online Natural Resources Information System database (<http://sonris.com/>, accessed March 2014). Texas well locations and natural gas production data were obtained from the Railroad Commission of Texas (RRC) Web site (<http://webapps2.rrc.state.tx.us/EWA/ewaPdqMain.do>, accessed November 2013). Arkansas well locations and natural gas production data were obtained from the State of Arkansas Oil and Gas Commission (http://www.aogc.state.ar.us/Fay_Shale_GIS_Intro.htm, accessed March 2014). Pennsylvania well locations and natural gas production data were obtained from the Pennsylvania Department of Environmental Protection (<https://www.paoilandgasreporting.state.pa.us/publicreports/Modules/DataExports/DataExports.aspx>, accessed March 2014).

Locations of known point sources of CH₄ were obtained from the 2012 EPA greenhouse gas (GHG) inventory Web site (<http://ghgdata.epa.gov/ghgp/main.do>, accessed November 2013). Some latitude-longitude coordinates in the 2012 EPA GHG inventory data set have been modified to match the locations determined using Google Earth imagery. Hybrid Single Particle Lagrangian Integrated Trajectory (HYSPPLIT) model back trajectories [Draxler and Rolph, 2013; <https://ready.arl.noaa.gov/HYSPLIT.php>] are used to check spatial and temporal uniformity of wind fields, and are run with the following settings: Meteorology, North American Mesoscale Forecast System, 12 km; Vertical motion, model vertical velocity. As discussed above and in Figure 1, shale gas production data were obtained from the EIA Web site. The average natural gas chemical composition from each region is determined from a 2009 U.S. Geological Survey (USGS) database (<http://energy.cr.usgs.gov/prov/og/index.htm>) for wells that lie within the study regions. County level cattle and calf populations were obtained from the U.S. Department of Agriculture (USDA) National Agriculture Statistics Service (NASS) (<http://www.nass.usda.gov>). Assuming the same cattle population distribution as the EPA GHG inventory, we estimate an average emission of 67.8 kg CH₄/yr per head from enteric fermentation. In cases where the NOAA P-3 flight track transects a county or parish, an apportionment based on geographical area is used to determine how many livestock are within the study region by scaling linearly the number of cattle and calves as a function of the county area. County-level manure emissions estimates were obtained from the National Renewable Energy Laboratory Web site (<http://maps.nrel.gov/biomass>) and were based on 2002 USDA data. We apportion the manure emissions geographically the same as for enteric fermentation.

4. Mass Balance Approach

The mass balance approach is used to estimate CH₄ fluxes [White *et al.*, 1976]. This technique uses the fact that emissions mix and disperse vertically and horizontally through the atmosphere as they are carried

downwind. The flux of the integrated emissions of a conserved tracer through a plane normal to the wind velocity should be constant as the plume moves downwind, so long as the wind field remains constant. We assume, and verify with measurements, that these CH₄ emission plumes mix downwind until they uniformly fill the depth of the PBL, at which point they continue to dilute horizontally with minimal detrainment into the overlying free troposphere. In this experiment, the NOAA P-3 aircraft characterized the upwind methane concentrations and transected emission plumes downwind of a targeted region to estimate CH₄ emissions from that region. We calculate the flux of a species X through a plane defined by an aircraft transect:

$$\text{flux} = v \cos(\alpha) \int_{z_0}^{z_1} \int_{-y}^y (X - X_{\text{bg}}) dy dz \quad (1)$$

where $v \cos(\alpha)$ is the magnitude of the component of the wind velocity normal to the flight track, z_0 is the ground level, z_1 is the adjusted mixing height discussed in detail below, $(X - X_{\text{bg}})$ is the enhancement of CH₄ above the tropospheric background, and y is the crosswind distance [White *et al.*, 1976].

This method of determining emission fluxes was found to be in good agreement with an EPA emission inventory of nitrogen oxide emissions from Birmingham, Alabama [Trainer *et al.*, 1995], with EPA continuous emissions monitoring measurements for nitrogen oxide emissions from power plants [Ryerson *et al.*, 1998], and with the California Air Resource Board's GHG inventory for CH₄ emissions from landfills [Peischl *et al.*, 2013]. This method is similar to the method used by Mays *et al.* [2009] to determine greenhouse gas emissions from Indianapolis, Indiana, and by Caulton *et al.* [2014] to determine CH₄ emissions from oil and gas operations and coal mining in southwestern Pennsylvania. The mass balance technique was also used to determine CH₄ emissions from oil and natural gas operations in the Uinta Basin [Karion *et al.*, 2013] in Utah and the Denver-Julesburg Basin [Pétron *et al.*, 2014] in Colorado.

We assume that the CH₄ emitted from a region is well mixed through the depth of the PBL by the time it is measured aboard the NOAA P-3. This assumption is tested with frequent vertical profiles, usually once or twice per hour, which also serve to assess the PBL depth. We further assume that the wind fields were constant between emission and measurement aboard the P-3; this assumption is verified using HYSPLIT back trajectories.

4.1. Determining Background CH₄ Mixing Ratios

We define the PBL background CH₄ mixing ratio, X_{bg} in equation (1), as the lowest mixing ratios encountered in the PBL during the upwind portions of the flights. Uncertainty in the background is defined as the atmospheric variability in the upwind values that are not immediately influenced by known upwind sources. As the PBL grows over the course of a flight, entrainment occurs between the free troposphere and the PBL, which mixes free tropospheric air into the PBL, and vice versa. We define the entrainment height, z_e , as the altitude above the PBL to which this mixing occurs, based on examination of vertical profiles, and define the entrainment zone as the portion of the atmosphere located between the top of the PBL and the entrainment height. We assume that the free tropospheric background level of CH₄ mixes with the PBL background proportional to the increase in the PBL depth, weighted by the number density of the atmosphere. We test this assumption by integrating the estimated background CH₄ from ground level to the maximum entrainment height noted on each flight, similar to Figure 2 of the work of Sasakawa *et al.* [2013], for each vertical profile. We linearly interpolate between the PBL CH₄ background and the free tropospheric CH₄ background through the entrainment zone for this vertical integration calculation. We refer to this interpolation as the entrainment zone CH₄ background. As the PBL grows during the course of a flight, the PBL CH₄ background is adjusted so that the vertically integrated CH₄ background remains constant to within 0.5 ppb.

4.2. Determining Planetary Boundary Layer Depth and Adjusted Mixing Height

We define the top of the PBL as the altitude of maximum virtual potential temperature gradient and corroborate this by examining gradients in CO, ambient temperature, wind speed and direction, and dew point temperature observed in vertical profiles. We further assume a constant mixing height above ground and estimate a ± 200 m uncertainty for the assigned PBL depth.

CH₄ enhancements may be transported vertically through the top of the PBL from shear-induced mixing, transport through clouds, or from PBL depth changes over time. We account for this by defining the adjusted mixing height, z_1 in equation (1), such that $z_1 > z_{\text{PBL}}$. As with the entrainment zone CH₄ background, we

assume constant linear mixing in the entrainment zone and therefore interpolate between the CH₄ enhancement in the PBL and the tropospheric background CH₄. The CH₄ enhancement over background in the PBL during a vertical profile is represented as the area of a rectangle, with a width of $(X - X_{bg})$ and a height of $(z_{PBL} - z_0)$. Likewise, the CH₄ enhancement over background in the entrainment zone is represented as the area of a triangle, with a base of $(X - X_{bg})$ and a height of $(z_e - z_{PBL})$. We therefore define the adjusted mixing height by increasing z_{PBL} by the additional fraction of one half the area of the triangle divided by the area of the rectangle:

$$z_1 = z_{PBL} \times \left\{ 1 + \frac{[(z_e - z_{PBL})(X - X_{bg})/4]}{[(z_{PBL} - z_0)(X - X_{bg})]} \right\} \quad (2)$$

The $(X - X_{bg})$ terms in equation (2) cancel, and $z_0 = 0$ as defined in units of meters above ground level (magl). Therefore, equation (2) simplifies to

$$z_1 = (3z_{PBL} + z_e)/4 \quad (3)$$

where the z terms are also defined in units of magl. We estimate the uncertainty of z_1 by summing in quadrature $(z_1 - z_{PBL})$ and 200 m. The result is an adjusted mixing height with uncertainties that encompass both z_{PBL} and the height of a rectangle with an area that represents the PBL CH₄ enhancements lost to detrainment.

Next, we fit a line to the adjusted mixing heights calculated for each vertical profile, weighted by the uncertainty in the adjusted mixing height. For each mass balance transect, z_1 in equation (1) is found by taking the mean of the fit during the time of the transect. In each instance, the 1σ confidence bar for the fit was $< \pm 200$ m. However, here we use a more conservative uncertainty estimate of ± 300 m, which encompasses all the adjusted mixing heights used in the fit.

We estimate uncertainties in the flux determination by quadrature addition of the uncertainties of each of the variables in equation (1). In the cases where the NOAA P-3 did not fly a complete upwind transect, we increase the estimated uncertainty of the background CH₄ mixing ratio to include the upwind variability of CH₄ in areas not immediately downwind of known point sources.

5. Results and Discussion

Five SENEX flights were conducted in regions with extensive unconventional shale gas production, with transects performed upwind, over, and downwind of these regions. Figure 2 shows three flight tracks of the NOAA P-3 to the regions of the Haynesville, Fayetteville, and the Marcellus shale plays in June and July 2013. Although the Marcellus shale formation is large, extending from New York through Pennsylvania and Ohio and into West Virginia, in 2013 the majority of unconventional natural gas production from the shale play was located in northeastern Pennsylvania. Using equation (1), we determine the CH₄ emission fluxes from these three regions. We then determine the natural gas loss rate from oil and gas operations in these regions by converting the CH₄ emission to a natural gas emission, then dividing this calculated natural gas emission by the total natural gas production in that region.

5.1. CH₄ Emissions to the Atmosphere From the Haynesville, Fayetteville, and Marcellus Study Regions

5.1.1. Haynesville

The NOAA P-3 aircraft flew to the Haynesville region on 10 June and 25 June 2013. For the 10 June flight, the wind field was not uniform throughout the Haynesville region; we therefore apply the mass balance technique only to data from the 25 June flight. On the 25 June flight, the winds measured aboard the P-3 were consistently from the south-southwest over the range of the study area, which agree with both HYSPLIT back trajectories and the location of plumes transected downwind of known point sources, such as the Martin Lake power plant.

A map of the 25 June flight shows that the box pattern flown by the NOAA P-3 encompassed the majority of the wells in the Haynesville region (Figure 3). The blue circles in Figure 3 show the locations of unconventional wells drilled into the Haynesville shale formation. The green circles show the locations of both conventional and unconventional active natural gas wells drilled into other geologic formations. Also shown in Figure 3 are CH₄ point sources in the EPA GHG inventory sized by their respective CH₄ emission. The flight track in Figure 3 is colored by the CH₄ mixing ratio measured within the PBL aboard the P-3 aircraft. These measurements show a general increase in CH₄ mixing ratios as the number of wells upwind increases. Black rectangles

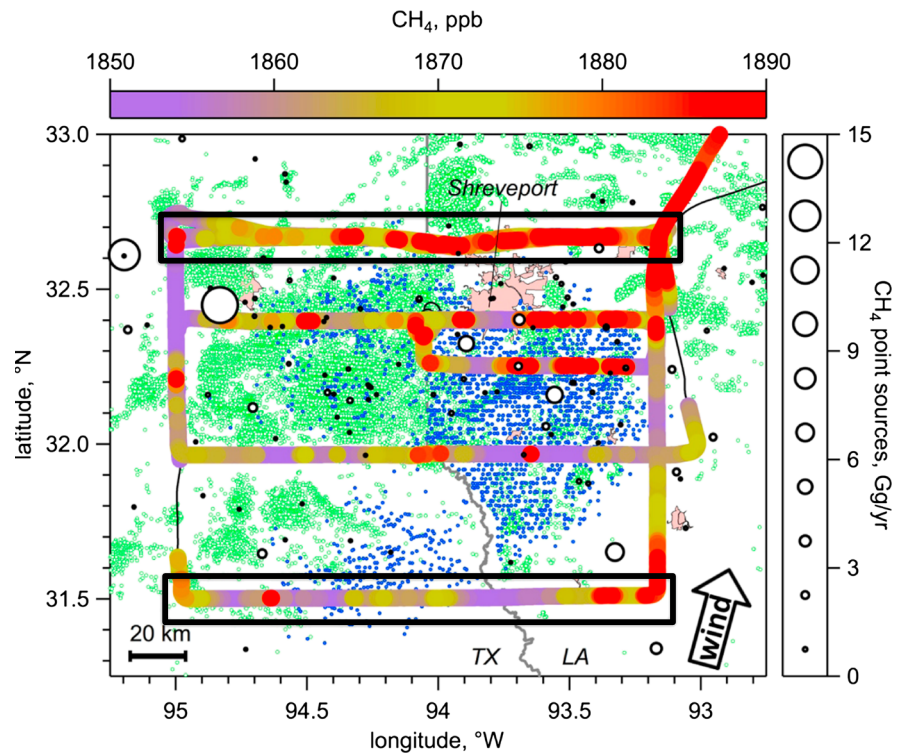


Figure 3. Map of the Haynesville shale region. The NOAA P-3 flight track from 25 June (black line) is colored by observed CH₄ mixing ratios in the boundary layer. Active unconventional gas wells drilled into the higher-production Haynesville shale formation are shown as blue circles. All other active gas wells are shown as green circles. Point sources from the 2012 EPA GHG inventory are shown as open black circles sized by inventory CH₄ emissions. Urban areas, including Longview, Texas, and Shreveport, Louisiana, are shaded pink. The black rectangles highlight the locations of the upwind transect along 31.5°N latitude and the three downwind transects along 32.7°N latitude.

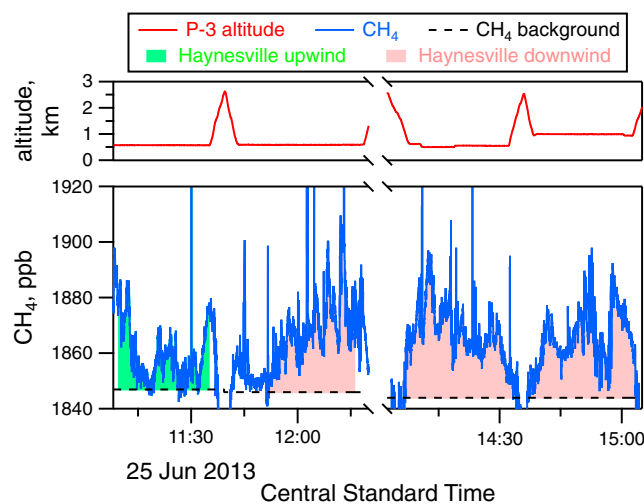


Figure 4. Time series of CH₄ measurements (blue) from the 25 June NOAA P-3 flight over the Haynesville study region. The red trace shows the P-3 altitude. The dashed black line indicates the background CH₄ mixing ratio, estimated at 1847 ppb for the upwind transect, 1846 ppb for the first downwind transect, and 1844 ppb for the final two downwind transects. The shaded areas show the CH₄ enhancement over background along the transect(s): upwind of the Haynesville region (green) and downwind of the Haynesville region (pink).

highlight the upwind transect at approximately 31.5°N latitude and the three downwind transects located at approximately 32.7°N latitude.

Figure 4 shows the time series of CH₄ and aircraft altitude for the one upwind and three downwind transects highlighted in Figure 3. Also plotted in Figure 4 is the estimate of the background CH₄ mixing ratio, which was adjusted to maintain a constant vertically integrated background as the PBL grew during the flight. We estimate an initial CH₄ background of 1847 ± 3 ppb for the upwind transect, 1846 ± 3 ppb for the first downwind transect, and 1844 ± 3 ppb for the final two downwind transects. Examples of the PBL depth estimates, determined using virtual potential temperature, ambient temperature, and dew point profiles, are shown for four vertical profiles in Figure 5. Figures 5a–5d show the vertical

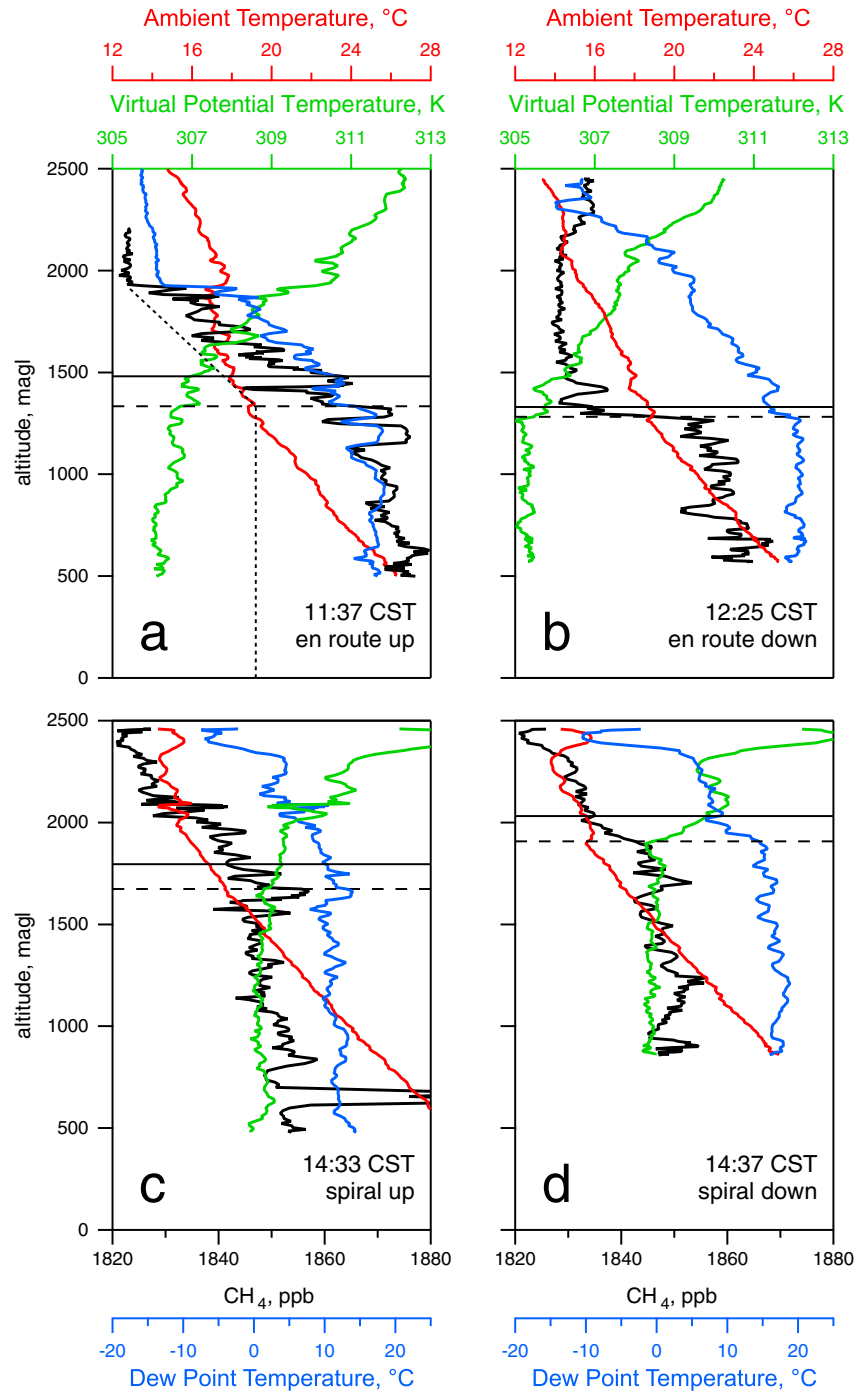


Figure 5. Four vertical profiles during the 25 June flight over the Haynesville study region. The vertical profiles immediately (a) after the upwind transect, (b) after the first downward transect, (c) after the second downward transect, and (d) before the third downward transect. Dashed lines indicate estimates of the well-mixed PBL depth. Solid lines indicate the adjusted mixing height, z_1 . The dotted line in (a) represents the background CH_4 mixing ratio throughout the vertical profile: the PBL background below the dashed line, the free tropospheric background above approximately 2.0 km, and a linear interpolation in the entrainment zone.

profiles immediately after the upwind transect, after the first downwind transect, after the second downwind transect, and before the third downwind transect, respectively. Figure 5a shows an example of how the adjusted mixing height is formulated for a vertical profile that indicates significant vertical CH_4 mixing above the PBL, possibly due to cumulus cloud formation. The dotted line in Figure 5a represents the estimated background CH_4 mixing ratio (i) in the PBL (dashed line), below 1334 magl, (ii) in the entrainment zone, between

Table 1. Example of Data Used in Equation (1) From the 25 June 2013 Flight to the Haynesville Shale Region

Side of Box	Terrain Height ^a (masl)	Adjusted Mixing Height (magl)	Wind Direction (deg)	Wind Speed (m/s)	Estimated CH ₄ Background (ppb)	CH ₄ Flux (10 ²⁶ molec./s)	CH ₄ Flux (10 ⁷ g/h) ^b
North, downwind #1	68 ± 21	1560 ± 300	204 ± 9	7.0 ± 1.8	1846 ± 3	9.5 ± 3.2	9.1 ± 3.1
North, downwind #2	75 ± 22	1791 ± 300	178 ± 11	6.5 ± 1.8	1844 ± 3	11.5 ± 3.9	11.0 ± 3.7
North, downwind #3	57 ± 23	1840 ± 300	190 ± 11	6.8 ± 1.8	1844 ± 3	11.0 ± 3.7	10.5 ± 3.5
East, downwind	44 ± 19	1429 ± 300	211 ± 10	5.4 ± 1.4	1847 ± 3	2.5 ± 0.9	2.4 ± 0.9
South, upwind	77 ± 22	1471 ± 300	192 ± 10	6.0 ± 1.6	1847 ± 3	-4.1 ± 1.6	-3.9 ± 1.6
West, upwind #1	92 ± 33	1541 ± 300	195 ± 7	8.4 ± 1.8	1846 ± 3	-0.3 ± 0.2	-0.3 ± 0.1
West, upwind #2	132 ± 23	1636 ± 300	182 ± 9	6.8 ± 1.8	1845 ± 3	-0.2 ± 0.1	-0.2 ± 0.1

^aMeters above sea level.^bA negative flux indicates an upwind transect, where the flux is into the region.

1334 and 1926 magl, and (iii) in the free troposphere, above 1926 magl. The area between the CH₄ trace and the dotted line in the entrainment zone is approximately 22% of the area between the CH₄ trace and the dotted line in the PBL, assuming that the average CH₄ mixing ratio in the PBL extends to the ground level, located at 77 m in this case. We therefore increase our estimated PBL depth, 1334 ± 200 magl, by approximately (11 ± 11)% to obtain the adjusted mixing height, 1482 ± 259 magl, for this vertical profile, which is indicated by the solid horizontal line in Figure 5a. We next fit a line to the adjusted mixing heights calculated for each vertical profile in order to estimate z_1 for the transects between vertical profiles. This results in adjusted mixing heights of 1471 ± 300 magl for the upwind transect immediately before the profile shown in Figure 5a, and 1541 ± 300 magl for the upwind transect shortly after the profile (Table 1). In Figure 5c, a plume of CH₄ was encountered at approximately 700 m during a spiral ascent. However, the P-3 was at or above the PBL when the aircraft would have encountered the plume farther downwind, so we cannot determine if the plume was well mixed vertically.

Table 1 lists the variables and their uncertainties used in equation (1) to calculate the CH₄ flux for each transect. For this flight, the largest drivers of the flux uncertainty were the wind speed, ±25%, and the mixing height, ±20%, whereas the ±3 ppb background uncertainty introduces only a ±6% flux uncertainty due to the fact that the upwind fluxes are subtracted from the downwind fluxes. The CH₄ fluxes calculated from the three downwind transects are $(9.1 ± 3.1) × 10^7$, $(11.0 ± 3.7) × 10^7$, and $(10.5 ± 3.5) × 10^7$ g CH₄/h, with a $1/σ^2$ weighted average of $(10.1 ± 2.0) × 10^7$ g CH₄/h. In addition, CH₄ was enhanced above background along the eastern transect at 93.2°W longitude in Figure 3. The CH₄ flux calculated from this transect was $(2.4 ± 0.9) × 10^7$ g CH₄/h (Table 1). The P-3 intercepted a small biomass burning plume along this transect, which constitutes a possible source of CH₄ unrelated to oil and gas operations. We account for this possible interference by assuming a CH₄/CO ratio of 2% in the biomass burning plume [Andreae and Merlet, 2001] and subtracting this CH₄ enhancement due to the biomass burning from the CH₄ measurement. The biomass burning plume contributed little to the CH₄ enhancement during this transect, accounting for less than 1% of the calculated CH₄ flux through the eastern transect. There were, however, significant CH₄ enhancements above background upwind of the Haynesville region. We estimate the flux of CH₄ along the upwind portion of the flight track (Figures 3 and 4) to be $-4.1 × 10^7$ g CH₄/h, where the negative sign indicates excess CH₄ above background flowing into the region. Additionally, we estimate the flux of excess CH₄ along the western portion of the box to be $-0.5 × 10^7$ g CH₄/h. This number is the sum of the fluxes calculated from the western transect (West, Upwind #1 in Table 1) plus a small portion of the transect along 32.0°N latitude between 94.93°W and 94.98°W longitude (West, Upwind #2 in Table 1) to account for when the P-3 was not in the boundary layer during a vertical profile. Although this is not a Lagrangian study, in which the air mass we measure upwind is the same as the one we measure downwind, the upwind transects provide the best estimate of CH₄ enhancements above background flowing into the Haynesville region. Figure 6 shows data from the upwind transect and the first downwind transect of the Haynesville region. Histograms of these data are provided to the right of Figure 6, along with box and whisker plots of the CH₄ mixing ratio distribution along the two transects. The distributions show a significant increase in the CH₄ mixing ratio downwind of the Haynesville region. Figure 6 also illustrates our reason for including the sides of the box in the flux calculation. The upwind CH₄ enhancements located between 140 and 160 km (Figure 6) enter, then immediately exit, the study region in the southeast corner of the flight track (Figure 3), thereby negating these upwind emissions. Therefore, accounting for all sides of the box pattern flown by the P-3, we estimate the total CH₄ emission from within the box as $(8.0 ± 2.7) × 10^7$ g CH₄/h, which is the value included in Table 2.

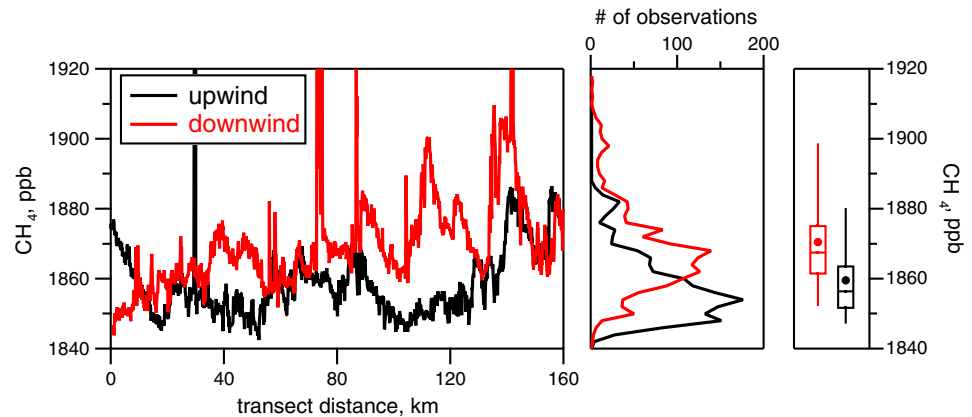


Figure 6. (left) CH₄ measurements upwind (black) and downwind (red) of the Haynesville study region. The downwind data shown are from the first of three downwind transects at 32.75°N latitude. (middle) Histograms for the data presented in Figure 6 (left). (right) The box and whisker plots of the data, where the top and bottom of the box are the 75th and 25th percentiles, respectively, and the tips of the whiskers represent the 95th and 5th percentiles. The closed circles represent the means.

5.1.2. Fayetteville and Western Arkoma

The NOAA P-3 aircraft flew to the Fayetteville region on 26 June and 8 July 2013. Due to active atmospheric mixing over mountainous terrain and a thunderstorm that forced the P-3 to leave the region prematurely, we do not interpret data from the 26 June flight. We apply the mass balance technique to data from the Fayetteville region for the 8 July flight only (Figure 7). During the 8 July 2013 flight, the winds measured aboard the P-3 were consistently out of the south-southwest in this region, which is supported by HYSPLIT back trajectories.

The area of study on 8 July can be split into two regions, roughly east and west of 92.8°W longitude. Although both regions are geologically part of the Arkoma Basin, there are different drilling strategies in these two regions. The Fayetteville shale play is represented by the large cluster of wells to the east (open blue circles in Figure 7), where the majority of unconventional drilling has occurred since 2010. The wells to the west are mostly conventional wells (green circles in Figure 7), and drilling in this region began in the early 1900s. Here we refer to the eastern part of the Arkoma Basin as the Fayetteville region and the western part of the Arkoma Basin in Arkansas as the Western Arkoma region. As in Figure 3, point sources from the 2012 EPA GHG inventory are shown as open black circles sized by their respective CH₄ emission in Figure 7, and the P-3 flight track is colored by CH₄ mixing ratio in the PBL.

The P-3 flew two transects downwind of the Fayetteville region along 35.7°N latitude and one upwind transect along 35.1°N latitude, between approximately 91.5° and 92.8°W longitude (Figures 7). We estimate the PBL CH₄ background mixing ratio, X_{bg} , at 1874 ppb for the initial downwind transect and at 1872 ppb for the later transects of the Fayetteville region. Although the CH₄ mixing ratios above the PBL on this flight were highly variable, ranging from 1850 to 1900 ppb, the adjustments to the PBL CH₄ background necessary to maintain a consistent vertically integrated CH₄ background were less than 1 ppb after 11 A.M. Central Standard Time, so we treat the effect of the entrained variability as negligible. We estimate a PBL background uncertainty of ± 3 ppb for the Fayetteville region. On this flight, the largest sources of uncertainty were the wind speed, ±35%, and the mixing height, ±25%. The CH₄ fluxes calculated from the two downwind transects are $(5.7 ± 2.4) × 10^7$ and

Table 2. Summary of CH₄ Emissions From Study Regions

Region	Haynesville	Western Arkoma	Fayetteville	Marcellus
CH ₄ flux (10 ⁷ g/h)	8.0 ± 2.7	3.3 ± 1.5	3.9 ± 1.8	1.5 ± 0.6
CH ₄ from livestock and non-oil-and-gas point sources (10 ⁷ g/h)	0.6	0.7	0.4	0.2
Natural gas production in June 2013 (10 ⁷ m ³ /d)	20 ± 3	0.9	7.6	18 ± 1
CH ₄ in natural gas	(90 ± 7)%	(95 ± 5)%	(94 ± 5)%	(96 ± 3)%
Natural gas loss rate	1.0–2.1%	6–20%	1.0–2.8%	0.18–0.41%

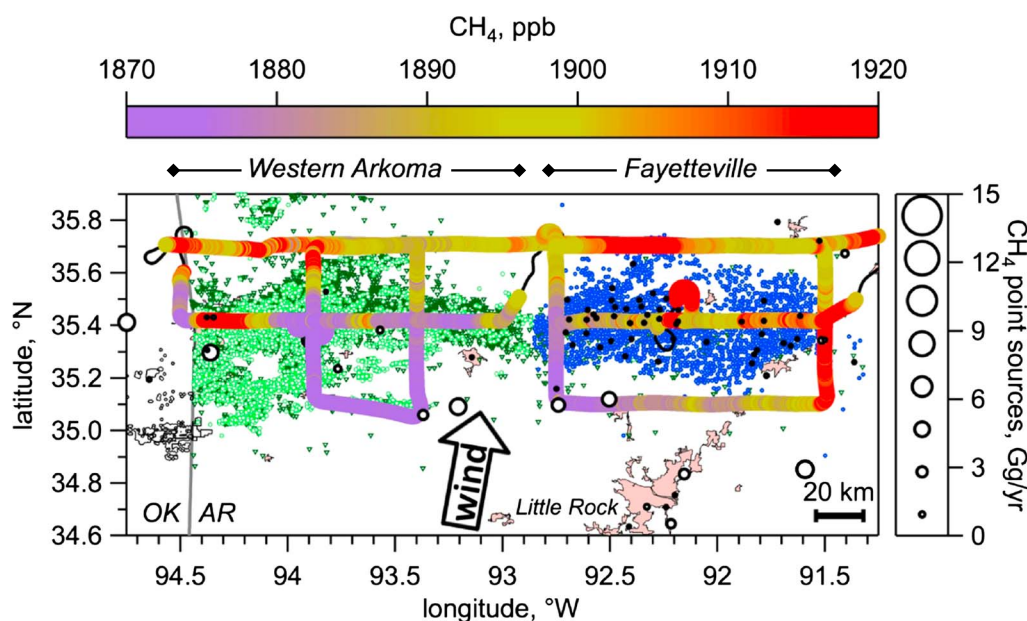


Figure 7. Map of the Fayetteville and Western Arkoma study regions. The NOAA P-3 flight track from 8 July (black line) is colored by observed CH_4 mixing ratios in the boundary layer. Active unconventional gas wells drilled into the Fayetteville shale formation are shown as blue circles. All other active gas wells are shown as green circles. Point sources from the 2012 EPA GHG inventory are shown as open black circles sized by inventory CH_4 emissions. Urban areas, including Little Rock, Arkansas, are shaded pink. Plugged gas wells are shown as dark green triangles. Coal bed methane fields are shown with thin black lines along the Arkansas-Oklahoma border.

$(4.6 \pm 2.0) \times 10^7$ g CH_4 /h (Figure 8). The weighted average flux is $(5.0 \pm 1.5) \times 10^7$ g CH_4 /h. However, the upwind transect shows some CH_4 enhancements, above the assigned CH_4 background, flowing into the region from the Little Rock urban area (Figure 8). Accounting for fluxes through all four sides of the box yields $(3.9 \pm 1.8) \times 10^7$ g CH_4 /h emitted from the Fayetteville region on 8 July (Figure 8 and Table 2).

We also calculate the CH_4 flux downwind of the Western Arkoma region using the downwind transect along 35.7°N latitude, between 92.8° and 94.5°W longitude (Figure 8). In this region, the P-3 did not fly a complete transect upwind of the active gas wells (Figure 7). As with the first transect downwind of the Fayetteville shale region, we estimate the background CH_4 mixing ratio at 1874 ppb. We account for unknown upwind CH_4 sources by increasing the uncertainty of the background to ± 5 ppb. The largest uncertainties for this transect were the wind speed, $\sim 30\%$, mixing height, $\sim 25\%$, and the background uncertainty, in this case, with no upwind transects, $\pm 20\%$. The CH_4 emission derived from the downwind transect is $(3.3 \pm 1.5) \times 10^7$ g CH_4 /h (Table 2).

5.1.3. Marcellus

The NOAA P-3 aircraft flew once to the Marcellus shale region in northeastern Pennsylvania on 6 July 2013 (Figure 9). Winds measured aboard the P-3 were consistently out of the west-southwest in this region for most of the flight in the boundary layer up until the last half hour of the flight, when they shifted to the southwest. The blue circles in Figure 9 show the locations of wells drilled into the Marcellus shale formation. The green open circles show the locations of conventional active natural gas wells. As in Figures 3 and 7, CH_4 point sources in the 2012 EPA GHG inventory are shown as open black circles sized by their respective CH_4 emission, and the flight track is colored by the CH_4 mixing ratio measured within the PBL.

The P-3 flew two sets of downwind transects on this day. The first was along 75.7°W longitude and then along 42°N latitude between 75.7° and 76.5°W longitude when the winds were from the south-southwest. The second was along 75.7°W longitude and then along 42°N latitude between 75.7° and 77.0°W longitude when the winds had shifted to the southwest. These sets of transects were downwind of nearly all the unconventional shale gas wells in this region. As with the Western Arkoma region, the P-3 did not fly a complete upwind transect on this day. Therefore, we assume a background CH_4 mixing ratio of 1862 ± 5 ppb for the first downwind transect, based on the lowest mixing ratios encountered in the PBL, and 1861 ± 5 ppb

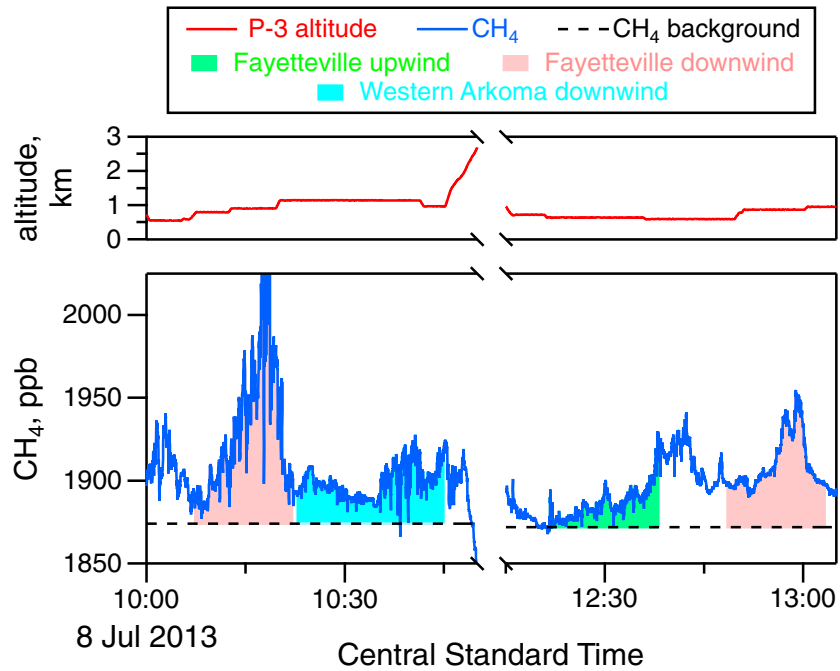


Figure 8. Time series of CH₄ measurements (blue) from the 8 July NOAA P-3 flight over the Fayetteville and Western Arkoma study regions. As in Figure 3, the red trace shows the P-3 altitude. The dashed black line indicates the background CH₄ mixing ratio, estimated at 1874 ppb for the first two downwind transects and 1872 ppb for the remaining transects. The shaded areas below the CH₄ trace show the CH₄ enhancement over background along the transect(s): upwind of the Fayetteville region (green), downwind of the Fayetteville region (pink), and downwind of the Western Arkoma region (light blue).

for the second downwind transect, estimated to maintain a constant vertically integrated CH₄ background (Figure 10). We then derive an upper limit to the CH₄ emissions from the region by applying the mass balance technique to the two sets of downwind transects. The largest sources of uncertainty on this flight were the wind speed, ±35%, the mixing height, ±20%, and the background, ±40%. The flux through the first set of

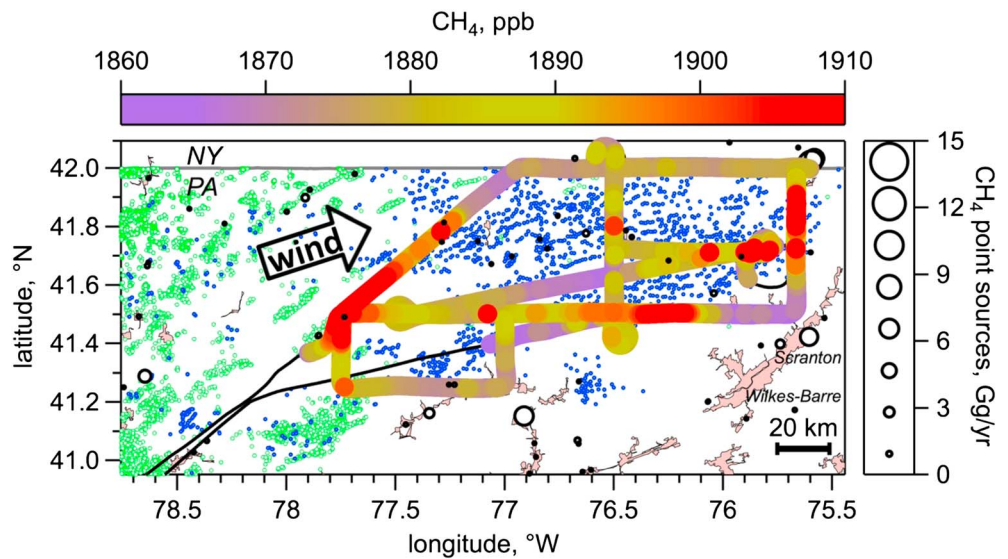


Figure 9. Map of the Marcellus study region in northeastern Pennsylvania. The NOAA P-3 flight track from 6 July (black line) is colored by observed CH₄ mixing ratios in the boundary layer. Active gas wells drilled into the Marcellus shale formation are shown as blue circles. All other active wells are shown as green circles. Point sources from the 2012 EPA GHG inventory are shown as open black circles sized by inventory CH₄ emissions. Urban areas are shaded pink.

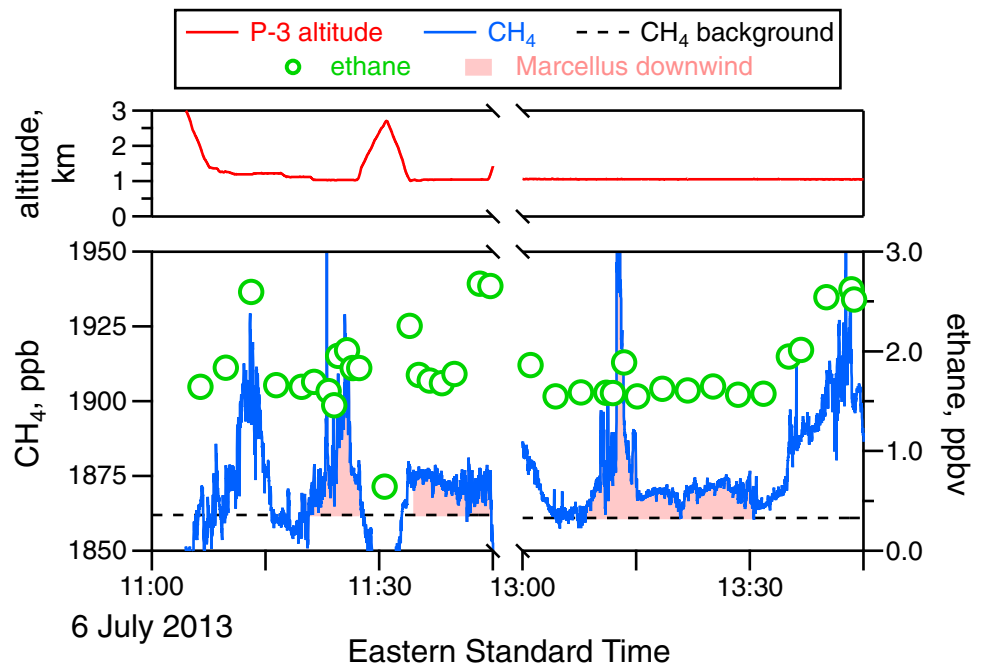


Figure 10. Time series of CH₄ measurements (blue) from the 6 July NOAA P-3 flight over the Marcellus shale region. As in Figures 3 and 7, the red trace shows the P-3 altitude. The dashed black line indicates the background CH₄ mixing ratio, estimated at 1862 ppb for the first set of downwind transects and 1861 ppb for the second. The shaded areas show the CH₄ enhancement over background along the transects downwind of the Marcellus region (pink). Observed ethane mixing ratios are plotted as open green circles.

downwind transects was $(1.3 \pm 0.7) \times 10^7$ g CH₄/h. The flux through the second set of downwind transects, after the winds had shifted slightly more to the southwest, was $(1.9 \pm 1.0) \times 10^7$ g CH₄/h. The weighted average of these two fluxes is $(1.5 \pm 0.6) \times 10^7$ g CH₄/h (Table 2).

5.2. Natural Gas Production in the Haynesville, Fayetteville, and Marcellus Study Regions

Monthly natural gas production in each of these three regions is estimated for the months of June and July from EIA data. Where possible, these production numbers are confirmed using state production data. We assume that daily natural gas production from these regions is equivalent to the monthly production divided by the number of days in the month of production. For ease of comparison between regions, we report all daily natural gas production figures in units of 10^7 m³.

5.2.1. Haynesville

The average Haynesville shale gas production for the month of June 2013 was 16×10^7 m³ (5.6 billion cubic feet) per day according to the EIA (Figure 1). We confirm the EIA production number using state production data. Production from the Louisiana portion of the Haynesville shale (fields with lease/unit/well name beginning with “HA” in the SONRIS database) was 3.5×10^9 m³ (123.8 billion cubic feet) for the month of June 2013, which averages to 12×10^7 m³/d. Production from wells drilled into the Texas portion of the Haynesville shale (the Carthage shale play, which is how the State of Texas refers to the Haynesville shale) for the month of June 2013 was 9.3×10^8 m³ (32.9 billion cubic feet), which averages to 3.1×10^7 m³ per day. Combined, these total to 15.1×10^7 m³/d, which is within 6% of the EIA production data.

However, natural gas production from geologic formations other than the Haynesville shale occurs in this region. We account for this additional production by using the state production data. In Louisiana, natural gas is extracted from other formations such as Cotton Valley and Hosston. In the eight-parish region encompassing the Haynesville shale play, total natural gas production was 4.2×10^9 m³ (148.1 billion cubic feet) in June 2013, which averages to 14×10^7 m³/d. Thus, the Haynesville shale accounted for 83% of the natural gas produced in the Louisiana portion of the Haynesville region. Similarly, in Texas, the total production from Gregg, Harrison, Nacogdoches, Panola, Rusk, and Shelby Counties, which were mostly

covered by the P-3 flight track, was $1.9 \times 10^9 \text{ m}^3$ (68.6 billion cubic feet) in June 2013, or $6.5 \times 10^7 \text{ m}^3/\text{d}$. Thus, the Haynesville shale accounted for approximately 48% of the natural gas produced in the Texas portion of the Haynesville region. The box bounded by the P-3 flight track in Figure 3 encompasses approximately 88% of the active Texas wells in the Texas RRC Oil and Gas Division District 6 (<http://www.rrc.state.tx.us/oil-gas/forms/maps/oil-gas-district-boundaries-map/>). Based on this apportioning, we assume $5.7 \times 10^7 \text{ m}^3$ natural gas per day was produced from the Texas portion of the Haynesville shale region. Combining the EIA, Louisiana, and Texas data, we estimate natural gas production of $(20 \pm 3) \times 10^7 \text{ m}^3/\text{d}$ from within the area bounded by the P-3 flight track on 25 June 2013 (Table 2).

5.2.2. Fayetteville and Western Arkoma

The average daily natural gas production from the Fayetteville shale play was $7.6 \times 10^7 \text{ m}^3$ (2.7 billion cubic feet) per day in July 2013 according to the EIA (Figure 1). In the State of Arkansas reports, the Fayetteville shale play is referred to as field B-43. According to the 2012 Annual Report of Production by the Arkansas Oil and Gas Commissioner, the B-43 field produced 1.0×10^9 thousands of cubic feet (MCF) of natural gas in 2012, or $2.8 \times 10^{10} \text{ m}^3$, which averages to $8.0 \times 10^7 \text{ m}^3/\text{d}$, the same number that the EIA provides for the Fayetteville shale play in 2012. The B-44 field, located in the Western Arkoma region, produced $6.4 \times 10^7 \text{ MCF}$, or $1.8 \times 10^9 \text{ m}^3$, of natural gas according to the 2012 Annual Report, which averages to $0.5 \times 10^7 \text{ m}^3/\text{d}$. Combined, these two fields produced 96% of the natural gas in northern Arkansas in 2012. This means that the wells represented by the green circles in Figure 7, which include those in the B-44 field in the Western Arkoma region and remaining wells not part of either the B-43 or B-44 fields, produced at most $0.9 \times 10^7 \text{ m}^3$ of natural gas per day on average in 2012. We therefore estimate a daily natural gas production rate of $7.6 \times 10^7 \text{ m}^3/\text{d}$ from the Fayetteville shale region using EIA data, and $0.9 \times 10^7 \text{ m}^3/\text{d}$ from the Western Arkoma region using EIA and State of Arkansas data (Table 2).

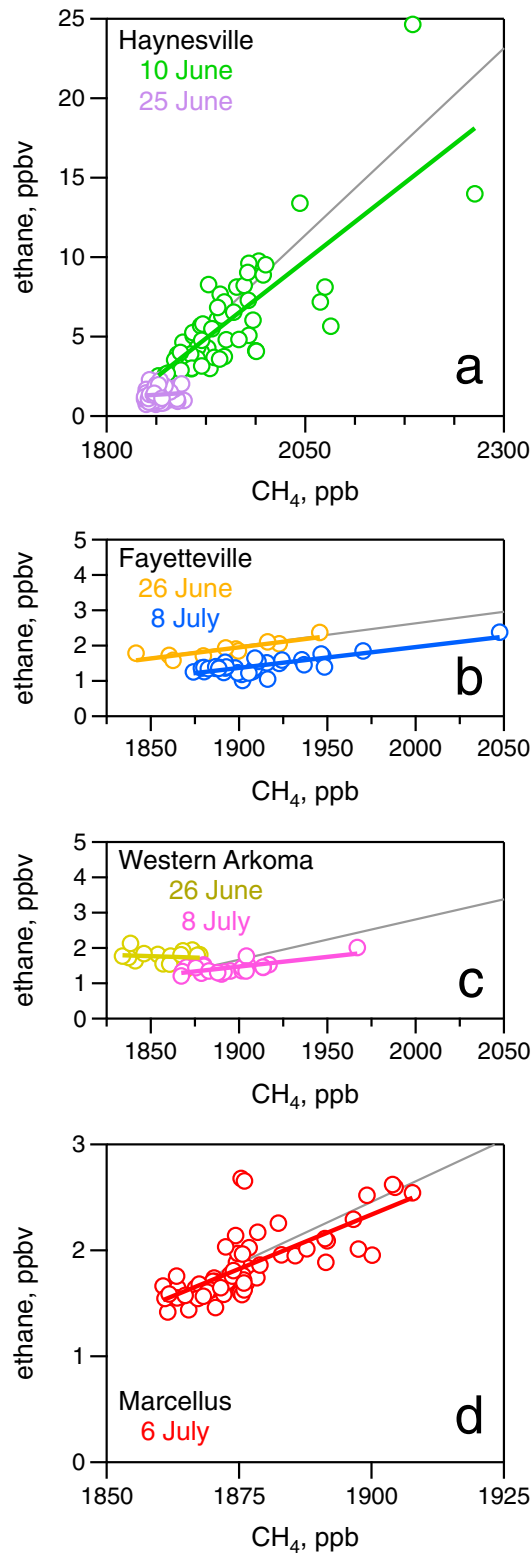
5.2.3. Marcellus

The Marcellus shale play produced $26 \times 10^7 \text{ m}^3$ (9.3 billion cubic feet) of natural gas per day in July 2013 according to the EIA (Figure 1). According to the State of Pennsylvania data, unconventional gas wells produced an average of $21 \times 10^7 \text{ m}^3/\text{d}$ from January to June 2013 and an average of $26 \times 10^7 \text{ m}^3/\text{d}$ from July to December 2013. If we assume an average of these two numbers that best represents the production for 6 July, when the NOAA P-3 flew to the area, then Marcellus shale gas production in Pennsylvania was approximately $24 \times 10^7 \text{ m}^3/\text{d}$, which is within a factor of 0.9 of the EIA production data. In contrast, production from conventional wells in Pennsylvania amounted to $1.6 \times 10^7 \text{ m}^3/\text{d}$ in 2013 or 7% that of the unconventional wells. The northern Pennsylvania portion accounted for about 73% of the Marcellus shale gas extracted in Pennsylvania in July 2013 (<http://www.eia.gov/todayinenergy/detail.cfm?id=12671>), although this northern Pennsylvania portion includes some areas of drilling outside the northeastern Pennsylvania study region for the 6 July flight. In 2012, the study region produced approximately 69% of the unconventional gas in Pennsylvania according to the Pennsylvania Department of Environmental Protection Web site. We therefore assume production from the northeastern Pennsylvania study region of (69 ± 3) percent of the total Marcellus shale gas production, which amounts to $(18 \pm 1) \times 10^7 \text{ m}^3$ of natural gas per day (Table 2).

5.3. Source Apportionment of CH₄ Emissions in the Haynesville, Fayetteville, and Marcellus Study Regions

Several arguments indicate that the oil and gas industry is the dominant source of CH₄ to the atmosphere of the Haynesville, Fayetteville, and Marcellus study regions. CH₄ enhancements were measured downwind of activity related to the oil and gas industry on scales ranging from individual point sources to the aggregate of wells on every flight to the Haynesville, Fayetteville, and Marcellus regions. Additionally, atmospheric ethane to CH₄ enhancement ratios measured by instruments aboard the P-3 aircraft in the PBL of each region are similar to the composition ratios in natural gas from that region (Figure 11), which indicates that natural gas is a dominant source of both alkanes to the atmosphere. Moreover, enhancement ratios of ethane, *n*-butane, and *i*-butane to propane in the PBL of the Haynesville and Fayetteville regions are similar to ratios in western oil and natural-gas-producing regions [e.g., Gilman *et al.*, 2013], while those in the PBL of the Marcellus region of northeastern Pennsylvania are similar to those reported by Caulton *et al.* [2014] for the Marcellus region of southwestern Pennsylvania.

Although natural gas emissions are believed to be the dominant source of CH₄ in these regions, other smaller contributing sources of CH₄ include agricultural emissions from livestock enteric fermentation and manure



management, point source emissions from landfills and wastewater treatment facilities, and other emissions from coal mines and leaks from natural gas distribution systems and end use. In the following sections, we compare inventory-based (or bottom-up) estimates of CH₄ emissions from point sources and livestock to the regionwide CH₄ emissions derived in section 5.1 to show that these source sectors are minor contributors to the overall CH₄ emissions. Additionally, we use NH₃ measurements aboard the P-3 to verify that enteric fermentation and manure management are not large sources of CH₄ in the three regions. Since NH₃ is coemitted with CH₄ from livestock, low NH₃ enhancements would indicate a minor livestock source of CH₄ to the regions studied here. Ultimately, because we cannot unambiguously attribute and quantify the agricultural emissions and the non-oil-and-gas point source emissions in the EPA GHG inventory using the measurements aboard the P-3, we instead treat these emissions as additional lower bound uncertainty in our analysis in section 5.4.

5.3.1. Haynesville

We attribute the largest CH₄ enhancements from the 25 June flight to emissions from the oil and gas industry. The CH₄ enhancements over background increase along the crosswind P-3 transects as the number of wells upwind increases (Figure 3). Further, the wells with the highest production of natural gas in the Haynesville region are located in an area to the south and southeast of Shreveport, Louisiana between approximately 32.1° and 32.5°N latitude, and the highest sustained measurements of CH₄ on 25 June were measured over and downwind of this same area (Figure 3). Additionally, CH₄ enhancements were measured immediately downwind of numerous point sources related to the oil and gas industry, such as gas plants and compressor stations. Finally, the boundary layer enhancement ratios of ethane to CH₄ determined from the slope of a one-sided regression fit, 0.039 ± 0.009 and 0.003 ± 0.004 ppbv ethane/ppb CH₄ on 10 and 25 June, respectively, agree within

Figure 11. Scatter plots of ethane versus CH₄ in the boundary layer for the (a) Haynesville, (b) Fayetteville, (c) Western Arkoma, and (d) Marcellus study areas. The colored lines are linear regression fits to the data. The gray lines represent the mean ratio of ethane to CH₄ in natural gas samples listed in the USGS database for each region. The shapes of the graphs maintain the same aspect ratio in the three panels, so that a direct comparison of the slopes can be made.

uncertainties with the highly variable ethane/CH₄ composition ratio in natural gas from the region in the USGS database, 0.047 ± 0.053 (Figure 11a).

Agricultural emissions. We estimate that the 25 June P-3 flight track in the Haynesville region encompassed 245,000 cattle and calves, based on a geographical apportionment of USDA NASS county and parish data. These livestock emit an estimated 1.9×10^6 g CH₄/h from enteric fermentation. CH₄ emissions from manure in this region are estimated at 0.6×10^6 g CH₄/h (<http://maps.nrel.gov/biomass>). We therefore estimate a total livestock emission of 2.5×10^6 g CH₄/h or only 3% of the total CH₄ emission of 8.0×10^7 g CH₄/h from the region calculated for this day. Mean NH₃ mixing ratio enhancements along the upwind and three downwind transects of this region were statistically no different from zero, and 1 Hz NH₃ measurements did not exceed 0.26 ppbv for the entire flight.

Point source emissions. The total CH₄ emission from point sources in the 2012 EPA GHG inventory not related to oil and natural gas processing in the Haynesville region is 38.4 Gg CH₄/yr, which scales to 4.4×10^6 g CH₄/h, or 5.5% of the CH₄ emission from this region assuming an average value applied to the 25 June flight. CH₄ was enhanced by approximately 10 ppb downwind of the largest point source, the Pinehill landfill located at 32.45°N latitude, 94.83°W longitude (Figure 3). However, these 1 min wide plumes, sampled at 11:55, 14:30, and 14:41 EST (Figure 4), did not stand out significantly from the surrounding CH₄ variability.

Other emissions. There are approximately 10 active surface coal mines in the Haynesville region, in addition to underground and abandoned mines. CH₄ was enhanced by up to 30 ppb directly downwind of several active coal mines surrounding the coal-fired Martin Lake power plant at 32.26°N latitude, 94.57°W longitude (Figure 3). However, by the farthest downwind transects, these emissions did not stand out above the CH₄ variability and thus did not contribute significantly to the derived flux ascribed to the Haynesville oil and gas operations. Additionally, there are two cities in the study region with metropolitan area populations greater than 200,000: Longview, Texas and Shreveport, Louisiana (Figure 3). Possible CH₄ sources from these urban areas include the distribution of natural gas to homes and hydrocarbon refining operations in Shreveport. Although we cannot quantify these emissions using P-3 data, we treat them as an additional lower bound uncertainty for our analysis in section 5.4. We combine the point source and other emissions uncertainty and estimate an additional 10% uncertainty for the lower bound of the loss rate from the Haynesville region in section 5.4.

5.3.2. Fayetteville and Western Arkoma

We attribute the largest CH₄ enhancements on the 8 July flight to the oil and gas industry in the Fayetteville region. As with the Haynesville region, the CH₄ enhancements increase as the crosswind P-3 transects move successively downwind of the Fayetteville wells (Figure 7). Additionally, the wells with the highest production of natural gas in the Fayetteville region are located in an area between 92.1°W longitude and 92.6°W longitude, and the highest sustained measurements of CH₄ on 8 July were located downwind of these wells (Figure 7). Finally, the boundary layer enhancement ratios of ethane to CH₄, 0.006 ± 0.002 ppbv ethane/ppb CH₄ for both flights, agree within uncertainties with the ethane/CH₄ composition ratio in natural gas from the region in the USGS database, 0.007 ± 0.003 (Figure 11b).

Agricultural emissions. We estimate that the 8 July flight track in the Fayetteville shale region encompassed 170,000 cattle and calves. This results in an estimated emission from enteric fermentation of 1.3×10^6 g CH₄/h. CH₄ emissions from manure in this region are estimated at 1.1×10^6 g CH₄/h (<http://maps.nrel.gov/biomass>). We therefore estimate a total livestock emission of 2.4×10^6 g CH₄/h, or only 6% of the total CH₄ emission of 3.9×10^7 g CH₄/h from the Fayetteville region calculated for this day. As with the Haynesville region, mean NH₃ mixing ratio enhancements along the upwind and two downwind transects of this region were statistically no different from zero, and 1 Hz NH₃ measurements averaged 0.1 ppbv over the Fayetteville region.

Point source emissions. The total CH₄ emission from point sources in the 2012 EPA GHG inventory not related to the oil and gas industry in the Fayetteville shale region is 8.0 Gg CH₄/yr, which scales to 0.9×10^6 g CH₄/h, or 2.3% of the CH₄ emission from this region. Emissions from two facilities, a paper manufacturing facility and a landfill, dominate the 2012 EPA GHG point source inventory and were both located along the southwestern edge of the 8 July flight path over the Fayetteville region (Figure 7). However, the emission plumes from these two point sources were lost in the CH₄ variability by the time the P-3 sampled them along the transect at 35.4°N latitude (Figure 7), suggesting a negligible contribution to the total CH₄ emission ascribed to Fayetteville oil and gas production.

Other emissions. There is no known coal mining activity in the Fayetteville region. Additionally, the flight track of 8 July did not encompass any large urban areas. We therefore treat these emissions as negligible for our analysis in section 5.4.

CH₄ enhancements also increase as the crosswind P-3 transects move successively downwind of the Western Arkoma wells (Figure 7). In addition to the approximately 4200 active gas wells, there are over 2500 plugged and abandoned gas wells in the Western Arkoma region. However, the largest sustained enhancements of CH₄ are located downwind of Fort Smith, Arkansas, located near 35.4°N latitude, 94.4°W longitude, and are attributed to emissions from a landfill and an unknown source, as discussed in more detail below.

Agricultural emissions. We estimate that the 8 July flight track encompassed 224,000 cattle and calves in the Western Arkoma region. This results in an estimated emission from enteric fermentation of 1.7×10^6 g CH₄/h. CH₄ emissions from manure in this region are estimated at 3.0×10^6 g CH₄/h. We therefore estimate a total livestock emission of 4.7×10^6 g CH₄/h or 14.5% of the total CH₄ emission of 3.3×10^7 g CH₄/h from the region calculated for this day. Livestock in the Western Arkoma region therefore account for the largest percentage of nonoil and gas CH₄ emissions from any of the oil and gas regions studied, which is further apparent from NH₃ measurements aboard the P-3. Mean NH₃ mixing ratio enhancements upwind of the Western Arkoma region were negligible, but 1 Hz NH₃ measurements were as high as 0.6 ppbv along the downwind transect and at times over 1 ppbv elsewhere in the region.

Point source emissions. The total CH₄ emission from point sources in the 2012 EPA GHG inventory not related to the oil and gas industry is 13.9 Gg CH₄/yr, which scales to 1.6×10^6 g CH₄/h or only 4.9% of the CH₄ emission from the Western Arkoma region. The largest of these point sources is the Fort Smith Sanitary Landfill, located at 35.30°N latitude, 94.36°W longitude (Figure 7). According to the inventory, this landfill emits 5.0 Gg CH₄/yr or an average of 5.7×10^5 g CH₄/h. The combined point source and livestock emissions, 5.9×10^6 g CH₄/h, comprise 19% of the total CH₄ emission from the region, the highest percentage for the oil and gas regions studied.

Other emissions. The NOAA P-3 sampled a CH₄ plume downwind of Fort Smith during both flights to the Western Arkoma region; a weighted average of the CH₄ flux derived from these two transects is $(5.1 \pm 1.7) \times 10^6$ g CH₄/h or a factor of approximately 10 greater than the 2012 EPA GHG inventory for the landfill. The crosswind extent (width) of the Fort Smith CH₄ plumes indicates either an area source larger than the landfill itself or an additional point source farther upwind of the landfill. Other possible sources contributing to the Fort Smith CH₄ plumes include active and plugged natural gas wells, active and abandoned coal mines, and coal bed methane production fields in Oklahoma (Figure 7). No whole air samples were taken in this particular plume on either flight day, so without corresponding ethane and propane data we cannot further identify the source of this CH₄ plume. However, it does account for 16% of the CH₄ emission calculated from this region. In addition to the plume downwind of Fort Smith, active coal mines are found throughout the Western Arkoma region (http://www.geology.ar.gov/energy/coal_geology.htm), but their contribution to the total CH₄ flux is not known. Finally, we do not estimate losses from natural gas distribution in Fort Smith, which has a metropolitan area population of nearly 300,000. We combine the livestock, point source, and other emissions to estimate an additional 35% uncertainty for the lower bound of the loss rate from the Western Arkoma region in section 5.4.

5.3.3. Marcellus

We attribute the largest CH₄ enhancements on the 6 July flight to the oil and gas industry. Although the P-3 did not fly a full upwind transect perpendicular to the prevailing wind direction, CH₄ enhancements were measured immediately downwind of numerous point sources related to the oil and gas industry, including compression stations and transmission stations. Additionally, the CH₄ enhancements measured during the flight were generally accompanied by ethane enhancements (Figure 10), indicating natural gas as the source of the majority of CH₄ emissions. Further, the boundary layer enhancement ratio of ethane to CH₄, 0.020 ± 0.005 ppbv ethane/ppbv CH₄, agrees within uncertainties with the ethane/CH₄ composition ratio of natural gas from the region in the USGS database, 0.023 ± 0.003 (Figure 11d). The highest levels of CH₄ and ethane were measured near 41.5°N latitude, 77.7°W longitude (Figure 9) at approximately 13:40 Eastern Standard Time (Figure 10). Three point sources related to either underground natural gas storage or natural gas transmission/compression in the EPA GHG inventory are located directly upwind of this location. However,

due to their location in the midst of conventional gas wells, this emission may not be associated with natural gas production from the Marcellus shale but rather from a conventional geologic formation.

Agricultural emissions. We estimate that the 6 July flight track in the Marcellus region encompassed 133,000 cattle and calves. This results in an estimated emission from enteric fermentation of 1.0×10^6 g CH₄/h. CH₄ emissions from manure in this region are estimated at 0.1×10^6 g CH₄/h. We therefore estimate a total livestock emission of 1.1×10^6 g CH₄/h or 8% of the total CH₄ emission of 1.5×10^7 g CH₄/h from the region calculated for this day. These emissions are consistent with minimal (<0.5 ppbv) enhancements in NH₃ measured aboard the aircraft in the region.

Point source emissions. The total CH₄ emission from point sources in the 2012 EPA GHG inventory not related to the oil and gas industry is 3.2 Gg CH₄/yr, which scales to 0.4×10^6 g CH₄/h, or only 2.5% of the total CH₄ emission calculated from this region. One point source upwind of the study area is the Veolia landfill located at 41.29°N latitude, 78.65°W longitude (Figure 9). However, we assume emissions from it and the wells surrounding it contributed to the background level of CH₄ found over the Marcellus unconventional shale wells (blue circles in Figure 9), thereby minimizing the affects of these emissions on our CH₄ flux calculations.

Other emissions. Although there are no large metropolitan areas in this region, there are coal mines in northeastern Pennsylvania which could contribute significantly to CH₄ emissions in the region. CH₄ enhancements were measured immediately downwind of one cluster of coal mines located at 41.5°N latitude, 76.4°W longitude (Figure 9). However, when the P-3 transected this area again later in the flight when the wind direction had shifted slightly to the southwest, CH₄ was enhanced upwind of the coal mines as well as downwind. We therefore attribute this CH₄ enhancement to the wells directly upwind of this area and neglect emissions from coal mines for our analysis in section 5.4.

5.4. Loss Rates to the Atmosphere From Natural Gas Production in the Haynesville, Fayetteville, and Marcellus Study Regions

Loss rates from natural gas operations in the three study regions are estimated by taking the derived CH₄ emission from a region, converting the mass emission to a volume of natural gas and dividing by the volume of natural gas produced in the region. The natural gas composition from each region is determined from the USGS database. The mean CH₄ abundance in these samples is shown in Table 2. These analyses are consistent with published works that provide composition analysis. For example, *Zumberge et al.* [2012] found that CH₄ accounted for 93–99% of all 101 natural gas samples taken from the Fayetteville shale, which compares well with the USGS database in which CH₄ averages $(94 \pm 5)\%$ in natural gas from the Fayetteville shale region. *Jackson et al.* [2013] found ethane to CH₄ ratios of less than 3% and propane to CH₄ ratios less than 1%, in every sample from 81 drinking water wells near the Marcellus shale formation, which suggests that CH₄ dominates the mix of alkanes similar to the USGS data set for northeastern Pennsylvania, where CH₄ accounts for $(96 \pm 3)\%$ of the natural gas. Because we use the EIA estimate for natural gas production, we therefore use the EIA standard 23.69 mol/L of natural gas in the conversion from mass to volume.

The natural gas loss rates from the Haynesville, Fayetteville, Western Arkoma, and Marcellus regions are shown in Table 2. *Howarth et al.* [2011] estimate that routine venting and equipment leaks lead to a loss of 0.3–1.9% of the CH₄ produced over the life cycles of both conventional and shale wells. The 1.0–2.1% and the 1.0–2.8% we report as loss rates from the Haynesville and Fayetteville study regions, respectively, are at the upper end of this range. The loss rate from the Marcellus study region, 0.18–0.41%, is at the lower end of this range. *Howarth et al.* [2011] estimated additional CH₄ emissions from well completions, liquid unloading, gas processing, and transport, storage, and distribution; however, we do not attempt to compare emissions from these activities at this time.

The CH₄ loss rate calculated for the Western Arkoma region, 6–20%, is most likely an overestimate. Emissions from livestock, point sources not related to the oil and gas industry, and a plume of unknown origin may account for one third of the CH₄ emissions in this region, which interferes with our assumption that all CH₄ emissions in a region come from the oil and gas industry. However, the high calculated loss rate does indicate that CH₄ emissions from inactive wells may be a significant source of CH₄ in this region.

The loss rate calculated for the Fayetteville region is similar to a study in an Arkansas Department of Environmental Quality report (http://www.adeq.state.ar.us/air/pdfs/fayetteville_shale_air_quality_report.pdf).

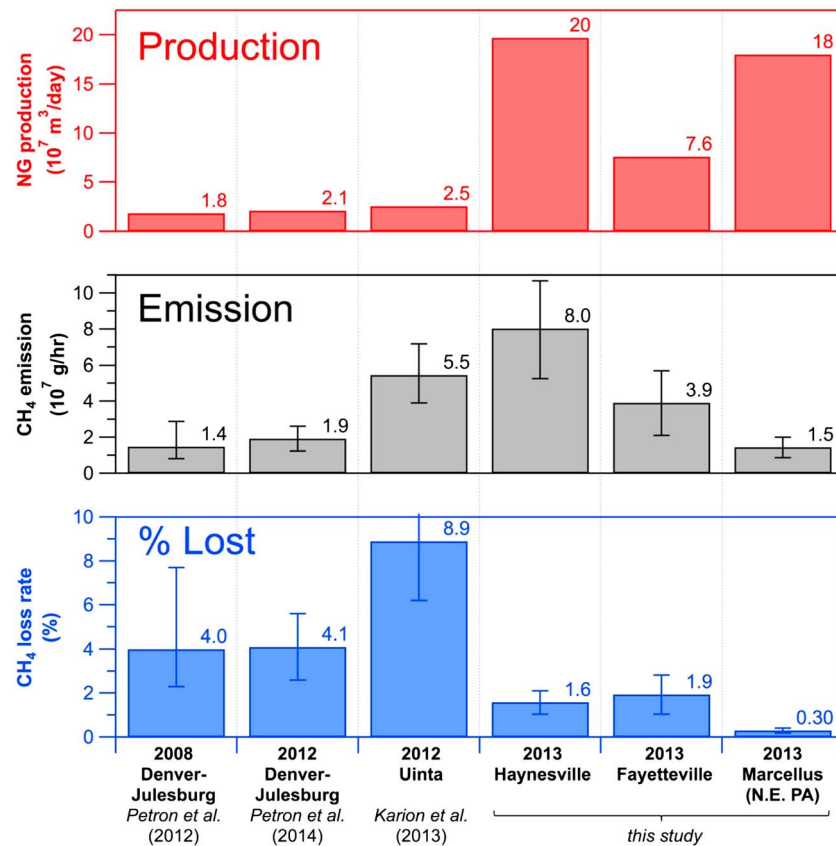


Figure 12. Summary of natural gas production, CH₄ emissions, and loss rates from oil and natural-gas-producing regions.

This study estimated a CH₄ emission from natural gas operations in the Fayetteville region in 2008 of 1.0×10^{11} g (112877 tons). Using 2008 EIA production data ($7.5 \times 10^9 \text{ m}^3$), this results in a loss rate of 2.0%, which is nearly identical to the loss rate we derive from a single flight in July 2013.

The production-weighted loss rate from the Haynesville, Fayetteville, and Marcellus study regions is 1.1%, which is similar to a loss rate calculated using the 2012 EPA GHG inventory and 2012 EIA natural gas production data. For this calculation, we assume that half the transmission and storage emissions from natural gas systems in the EPA GHG inventory occur in production regions, and half occur in distribution regions. Therefore, CH₄ emissions from the production side of natural gas systems in the 2012 EPA GHG inventory sum to 3920 GgCH₄/yr. According to the EIA, natural gas production from gas, shale gas, and coal bed wells totaled $7.0 \times 10^{11} \text{ m}^3$ in 2012. Assuming an 80% abundance of CH₄ in natural gas, the 2012 EPA emission/EIA production loss rate equals 1.0%.

The CH₄ emissions derived here are comparable in magnitude to CH₄ emissions from the Denver-Julesburg and Uinta basins (Figure 12) [Pétron et al., 2012, 2014; Karion et al., 2013]. However, due to the significantly larger natural gas production, the loss rates derived from the Haynesville, Fayetteville, and Marcellus study regions are significantly lower than those studies. One reason for this may be the composition of the fossil fuel extracted. There is less oil relative to natural gas produced from the Haynesville, Fayetteville, and Marcellus shale plays than there are from the Denver-Julesburg and Uinta basins. Further, the new-well gas production rate per drill rig has steadily increased since the late 2000s. Both improved technology and the exploration of new regions may play a role in this increased production efficiency. For example, the new-well gas production per rig was approximately a factor of 1.75 greater in the Marcellus region than in the Haynesville region for June and July 2013 (<http://www.eia.gov/petroleum/drilling/>), which may partly explain the lower loss rate found in the northeastern Pennsylvania portion of the Marcellus region.

6. Conclusions

We calculate 1 day CH₄ fluxes from three regions of unconventional shale gas production for early summer 2013, and find CH₄ emissions to the atmosphere of $(8.0 \pm 2.7) \times 10^7$ g/h from the Haynesville shale region in Louisiana and Texas, $(3.9 \pm 1.8) \times 10^7$ g/h from the Fayetteville shale region in Arkansas, and $(1.5 \pm 0.6) \times 10^7$ g/h from the Marcellus shale region in northeastern Pennsylvania. We derive loss rates as a percentage of natural gas production in the ranges of 1.0–2.1% from the Haynesville study region, 1.0–2.8% from the Fayetteville study region, and 0.18–0.41% from the Marcellus study region in northeastern Pennsylvania. Airborne measurements of NH₃ and a bottom-up inventory both indicate that livestock are not a large source of CH₄ to the atmosphere in these regions nor are landfills and other CH₄ point sources not related to the oil and gas industry in the 2012 EPA GHG inventory. Combined, livestock and these point sources account for approximately 10% of the total CH₄ emissions in each of the Haynesville, Fayetteville, and Marcellus study regions.

The natural gas loss rates from the Haynesville, Fayetteville, and Marcellus study regions are within the range of emissions estimated by Howarth *et al.* [2011] from the routine venting and equipment leaks of shale gas wells of 0.3–1.9%, which would represent the minimum day-to-day emission from a production region. In addition, the loss rates are lower than the threshold set by Alvarez *et al.* [2013] of 3.2%, below which the climate impact of using natural gas as a fuel in power plants would be less than that of coal. However, losses during the transmission and end-use stages will determine whether natural gas from these regions ultimately fall below the Alvarez *et al.* [2013] threshold. Yet, to our knowledge, this is the first airborne mass balance study in which CH₄ emissions from natural-gas-producing regions are below 3.2%. Further, the Haynesville, Fayetteville, and northeastern Pennsylvania Marcellus regions accounted for approximately 20% of U.S. natural gas production, and over 50% of unconventional shale gas production, at the time of the study. The production-weighted loss rate from the three regions is 1.1%. This rate is similar to a 1.0% loss rate derived from the 2012 EPA GHG emissions inventory for natural gas systems and 2012 EIA natural gas production numbers.

Finally, the magnitude of CH₄ emissions from the Haynesville, Fayetteville, and northeastern Pennsylvania Marcellus regions are comparable to those calculated from the Denver-Julesburg Basin in Colorado and the Uinta Basin in Utah, despite greater natural gas production from the former regions. Repeated measurements will be necessary to determine whether the 1 day CH₄ emission rates for the regions studied here are fully representative of those regions, to determine whether the CH₄ emission rates change over the full life cycle of fossil fuel production from each formation, and to understand the drivers behind regional differences in loss rates, of a factor of 20, now reported in the literature for different oil and gas-producing regions.

Acknowledgments

Data will be publicly available at <http://esrl.noaa.gov/csd/groups/csd7/measurements/2013senex/P3/DataDownload/> in July 2015. Until such time, data are available upon request. J.B.G. and B.M.L. thank NOAA Hollings Scholar M. Dumas and Hendrix College for partially funding A. Jacksich, D. Hughes, and C. D. Hatch, who helped with whole air sample measurements.

References

- Allen, D. T., et al. (2013), Measurements of methane emissions at natural gas production sites in the United States, *Proc. Natl. Acad. Sci. U.S.A.*, *110*, 17,768–17,773, doi:10.1073/pnas.1304880110.
- Alvarez, R. A., S. W. Pacala, J. J. Winebrake, W. L. Chameides, and S. P. Hamburg (2012), Greater focus needed on methane leakage from natural gas infrastructure, *Proc. Natl. Acad. Sci. U.S.A.*, *109*, 6435–6440, doi:10.1073/pnas.1202407109.
- Andreae, M. O., and P. Merlet (2001), Emission of trace gases and aerosols from biomass burning, *Global Biogeochem. Cycles*, *15*(4), 955–966, doi:10.1029/2000GB001382.
- Cathles, L. M., III, L. Brown, M. Taam, and A. Hunter (2012), A commentary on “The greenhouse-gas footprint of natural gas in shale formations” by R. W. Howarth, R. Santoro, and Anthony Ingraffea, *Clim. Change*, *113*, 525–535, doi:10.1007/s10584-011-0333-0.
- Caulton, D. R., et al. (2014), Toward a better understanding and quantification of methane emissions from shale gas development, *Proc. Natl. Acad. Sci. U.S.A.*, *111*(17), 6237–6242, doi:10.1073/pnas.1316546111.
- Colman, J. J., A. L. Swanson, S. Meinardi, B. C. Sive, D. R. Blake, and F. S. Rowland (2001), Description of the analysis of a wide range of volatile organic compounds in whole air samples collected during PEM-tropics A and B, *Anal. Chem.*, *73*(15), 3723–3731, doi:10.1021/ac10027g.
- Draxler, R. R., and G. D. Rolph (2013), HYSPLIT (Hybrid Single-Particle Lagrangian Integrated Trajectory) Model, access via NOAA ARL READY, NOAA Air Resources Laboratory, College Park, Md. [Available at <http://www.arl.noaa.gov/HYSPLIT.php>.]
- Gilman, J. B., B. M. Lerner, W. C. Kuster, and J. A. de Gouw (2013), Source signature of volatile organic compounds from oil and natural Gas operations in northeastern Colorado, *Environ. Sci. Technol.*, *47*, 1297–1305, doi:10.1021/es304119a.
- de Gouw, J. A., D. D. Parrish, G. J. Frost, and M. Trainer (2014), Reduced emissions of CO₂, NO_x, and SO₂ from U.S. power plants owing to switch from coal to natural gas with combined cycle technology, *Earth's Future*, *2*, 75–82, doi:10.1002/2013EF000196.
- Hayhoe, K., H. S. Keshgi, A. K. Jain, and D. J. Wuebbles (2002), Substitution of natural gas for coal: Climatic effects of utility sector emissions, *Clim. Change*, *54*, 107–139, doi:10.1023/A:1015737505552.
- Holloway, J. S., R. O. Jakoubek, D. D. Parrish, C. Gerbig, A. Volz-Thomas, S. Schmitgen, A. Fried, B. Wert, B. Henry, and J. R. Drummond (2000), Airborne intercomparison of vacuum ultraviolet fluorescence and tunable diode laser absorption measurements of tropospheric carbon monoxide, *J. Geophys. Res.*, *105*(D19), 24,251–24,261, doi:10.1029/2000JD900237.
- Howarth, R. W., R. Santoro, and A. Ingraffea (2011), Methane and the greenhouse-gas footprint of natural gas from shale formations, *Clim. Change*, *106*, 679–690, doi:10.1007/s10584-011-0061-5.

- Jackson, R. B., A. Vengosh, T. H. Darrah, N. R. Warner, A. Down, R. J. Poreda, S. G. Osborn, K. Zhao, and J. D. Karr (2013), Increased stray gas abundance in a subset of drinking water wells near Marcellus shale gas extraction, *Proc. Natl. Acad. Sci. U.S.A.*, *110*, 11,250–11,255, doi:10.1073/pnas.1221635110.
- Karion, A., et al. (2013), Methane emissions estimate from airborne measurements over a western United States natural gas field, *Geophys. Res. Lett.*, *40*, 4393–4397, doi:10.1002/grl.50811.
- Mays, K. L., P. B. Shepson, B. H. Stirm, A. Karion, C. Sweeney, and K. R. Gurney (2009), Aircraft-based measurements of the carbon footprint of Indianapolis, *Environ. Sci. Technol.*, *43*(20), 7816–7823.
- Myhre, G., et al. (2013), Anthropogenic and natural radiative forcing, in *Climate Change 2013: The Physical Science Basis. Contribution of Working Group I to the Fifth Assessment Report of the Intergovernmental Panel on Climate Change*, edited by T. F. Stocker et al., p. 714, Cambridge Univ. Press, Cambridge, U. K., and New York.
- Nowak, J. B., J. A. Neuman, K. Kozai, L. G. Huey, D. J. Tanner, J. S. Holloway, T. B. Ryerson, G. J. Frost, S. A. McKeen, and F. C. Fehsenfeld (2007), A chemical ionization mass spectrometry technique for airborne measurements of ammonia, *J. Geophys. Res.*, *112*, D10S02, doi:10.1029/2006JD007589.
- Peischl, J., et al. (2012), Airborne observations of methane emissions from rice cultivation in the Sacramento Valley of California, *J. Geophys. Res.*, *117*, D00V25, doi:10.1029/2012JD017994.
- Peischl, J., et al. (2013), Quantifying sources of methane using light alkanes in the Los Angeles basin, California, *J. Geophys. Res. Atmos.*, *118*, 4974–4990, doi:10.1002/jgrd.50413.
- Pétron, G., et al. (2012), Hydrocarbon emissions characterization in the Colorado Front Range: A pilot study, *J. Geophys. Res.*, *117*, D04304, doi:10.1029/2011JD016360.
- Pétron, G., et al. (2014), A new look at methane and nonmethane hydrocarbon emissions from oil and natural gas operations in the Colorado Denver–Julesburg Basin, *J. Geophys. Res. Atmos.*, *119*, 6836–6852, doi:10.1002/2013JD021272.
- Ryerson, T. B., et al. (1998), Emissions lifetimes and ozone formation in power plant plumes, *J. Geophys. Res.*, *103*(D17), 22,569–22,583, doi:10.1029/98JD01620.
- Sasakawa, M., T. Machida, N. Tsuda, M. Arshinov, D. Davydov, A. Fofonov, and O. Krasnov (2013), Aircraft and tower measurements of CO₂ concentration in the planetary boundary layer and the lower free troposphere over southern taiga in West Siberia: Long-term records from 2002 to 2011, *J. Geophys. Res. Atmos.*, *118*, 9489–9498, doi:10.1002/jgrd.50755.
- Trainer, M., B. A. Ridley, M. P. Buhr, G. Kok, J. Walega, G. Hübler, D. D. Parrish, and F. C. Fehsenfeld (1995), Regional ozone and urban plumes in the southeastern United States: Birmingham, a case study, *J. Geophys. Res.*, *100*(D9), 18,823–18,834, doi:10.1029/95JD01641.
- U.S. Environmental Protection Agency (2014), Inventory of U.S. greenhouse gas emissions and sinks: 1990–2012, Report # EPA 430-R-14-003. [Available at <http://www.epa.gov/climatechange/ghgemissions/usinventoryreport.html>.]
- White, W. H., J. A. Anderson, D. L. Blumenthal, R. B. Husar, N. V. Gillani, J. D. Husar, and W. E. Wilson Jr. (1976), Formation and transport of secondary air pollutants: Ozone and aerosols in the St. Louis urban plume, *Science*, *194*, 187–189, doi:10.1126/science.959846.
- Wigley, T. M. L. (2011), Coal to gas: The influence of methane leakage, *Clim. Change*, *108*, 601–608, doi:10.1007/s10584-011-0217-3.
- Yamartino, R. J. (1984), A comparison of several “single-pass” estimators of the standard deviation of wind direction, *J. Clim. Appl. Meteorol.*, *23*, 1362–1366.
- Zumberge, J., K. Ferworn, and S. Brown (2012), Isotopic reversal (‘rollover’) in shale gases produced from the Mississippian Barnett and Fayetteville formations, *Mar. Pet. Geol.*, *31*, 43–52, doi:10.1016/j.marpetgeo.2011.06.009.

Erratum

In the originally published version of this article, Figure 5 contained errors. These errors have since been corrected and this version may be considered the authoritative version of record.